CO₂ Reduction

International Edition: DOI: 10.1002/anie.201506961
German Edition: DOI: 10.1002/ange.201506961

Striking Differences in Properties of Geometric Isomers of [Ir(tpy)(ppy)H]$^+$: Experimental and Computational Studies of their Hydricities, Interaction with CO_2, and Photochemistry

Komal Garg, Yasuo Matsubara, Mehmed Z. Ertem, Anna Lewandowska-Andralojc, Shunsuke Sato, David J. Szalda, James T. Muckerman, and Etsuko Fujita**

***Abstract:** We prepared two geometric isomers of [Ir(tpy)(ppy)H]$^+$, previously proposed as a key intermediate in the photochemical reduction of CO_2 to CO, and characterized their notably different ground- and excited-state interactions with CO_2 and their hydricities using experimental and computational methods. Only one isomer, C-trans-[Ir(tpy)(ppy)H]$^+$, reacts with CO_2 to generate the formato complex in the ground state, consistent with its calculated hydricity. Under photocatalytic conditions in CH_3CN/TEOA, a common reactive C-trans-[Ir(tpy)(ppy)]^0 species, irrespective of the starting isomer or monodentate ligand (such as hydride or Cl), reacts with CO_2 and produces CO with the same catalytic efficiency.*

The photochemical reduction of CO_2 to useful chemicals such as CO, formic acid, or methanol has gathered significant attention during the last several decades owing to problems related to the depletion of fossil fuels and global warming.[1] Despite the challenges associated with the high thermodynamic and kinetic stability of CO_2, a number of photocatalytic systems have been investigated with transition metal polypyridyl complexes[2] as photosensitizers and as catalysts/precatalysts together with sacrificial electron donors. Typical products of photochemical CO_2 reduction are CO and formate, which have been proposed to form through metal-carboxylate and metal-hydride intermediates, respectively, however in some cases proton reduction to H_2 is a competing reaction.

Sato et al. recently reported an efficient photocatalytic system with [Ir(tpy)(ppy)Cl]$^+$ (Ir(tpy)(ppy) = complex **1**, tpy = 2,2′:6′,2″-terpyridine, ppy = 2-phenylpyridine) and triethanolamine (TEOA) in CH_3CN that selectively reduces CO_2 to CO under visible light ($410 < \lambda < 750$ nm) with a TON of 38 and quantum yield (Φ_{CO}) of 0.13.[3] This system is twice as efficient as the well-known [Re(bpy)(CO)$_3$Cl] system under the given conditions.[3] The proposed catalytic cycle includes the formation of the one-electron-reduced (OER) species, followed by the loss of the coordinated Cl^- and the formation of the hydride species with further reduction. While [**1**-H]$^+$ was detected by ^{1}H NMR during the photocatalytic reaction, it does not react with CO_2 in its ground state. Therefore, the further reduced species produced by its photoreduction was considered to react with CO_2 to form a CO_2 adduct, followed by the removal of CO.[3] Although the isolation of the hydride complex was mentioned, no synthetic or mechanistic details were provided regarding the reactivity of the hydride.

More recently, Reithmeier et al. have developed mononuclear Ir^{III} photocatalysts [Ir(tpy)(mppy)Cl]$^+$ (mppy = 4-methyl-2-phenylpyridine) and the dinuclear analogues with bis(2-phenylpyridin-4-yl) bridges for photo-induced CO_2 reduction.[4] They proposed the involvement of five-coordinate [Ir(tpy)(mppy)]$^{+/0}$ without any hydrides. Because the involvement of Ir-hydride intermediates in photochemical CO_2 reduction is not clear, we believe that a more complete understanding of Ir-hydride intermediates is important for the rational development of new catalysts for CO_2 reduction/CO_2 hydrogenation. Here we have isolated two isomers of [**1**-H]$^+$, where the hydride is trans to either N of ppy (*N-trans*-[**1**-H]$^+$) or to C of ppy (*C-trans*-[**1**-H]$^+$; Scheme 1), and have studied their distinct reactivity in the ground and excited states. We also report on the comparison of the hydricity of the two isomers and its relation to their CO_2 reduction through theoretical and experimental investigations. In fact, the hydricity is an important concept in the reduction of CO_2 beyond CO and formate.[5,6]

Two hydride isomers, *N-trans*-[**1**-H]$^+$ and *C-trans*-[**1**-H]$^+$, were prepared by a modification of the published procedures[7] for [Ru(tpy)(ppy)H]$^+$ and are described in detail in the Supporting Information. The final yield of *N-trans*-[**1**-H]$^+$ was low (ca. 10%) owing to the formation of a hydride-bridged iridium dimer, *C-trans*-[**1**-H-**1**]$^{3+}$, taking place as a side reaction. *C-trans*-[**1**-H]$^+$ is more difficult to synthesize on a large scale owing to its conversion to the more stable *N*-

---

[*] Dr. K. Garg,[+] Dr. Y. Matsubara,[$] [+] Dr. M. Z. Ertem,
Dr. A. Lewandowska-Andralojc,[#] Dr. J. T. Muckerman, Dr. E. Fujita
Chemistry Department, Brookhaven National Laboratory
Upton, NY 11973-5000 (USA)
E-mail: mzertem@bnl.gov
fujita@bnl.gov

Dr. Y. Matsubara,[$] [+] Dr. S. Sato
PRESTO, JST
4-1-8 Honcho, Kawaguchi, Saitama 332-0012 (Japan)

Dr. S. Sato
Toyota Central R & D Labs, Inc.
Nagakute, Aichi, 480-1192 (Japan)

Dr. D. J. Szalda
Department of Natural Science,
Baruch College, CUNY, New York, NY 10010 (USA)

[$] Present address: Kanagawa University
Rokkakubashi 3-27-1, Kanagawa-ku, Yokohama 221-8686 (Japan)

[#] Present address: Faculty of Chemistry, Adam Mickiewicz University
Umultowska 89b, 61614 Poznan (Poland)

[+] These authors contributed equally to this work.

Supporting information for this article is available on the WWW under http://dx.doi.org/10.1002/anie.201506961.

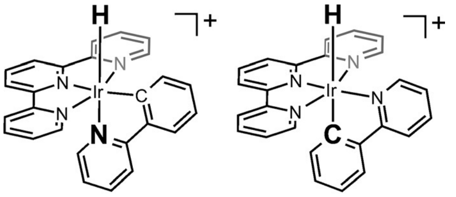

N-trans-[**1**–H]$^+$ *C-trans*-[**1**–H]$^+$

Scheme 1. Geometric isomers of [Ir(tpy)(ppy)H]$^+$.

trans-[**1**-H]$^+$ and the formation of the *C-trans*-[**1**-H-**1**]$^{3+}$ dimer during the synthesis. The μ-H chemical shift was observed at −11.4 ppm (Supporting Information, Figure S1), and Ir-H signals for *N-trans*- and *C-trans*-[**1**-H]$^+$ were found at −19.3 and −7.46 ppm, respectively (Supporting Information, Figures S2, S3). The X-ray structure of *N-trans*-[**1**-H](PF$_6$) has been determined (Supporting Information, Figures S4, S5) and selected bond distances and angles are summarized together with calculated ones at the M06 level of theory[8] for both geometric isomers (Supporting Information, Table S2 and Computational Methods). It should be noted that the calculated Ir-H distance in *C-trans*-[**1**-H]$^+$ is 0.11 Å longer than that in *N-trans*-[**1**-H]$^+$ as expected owing to the stronger *trans* influence in the former. The hydride isomers exhibit different absorption spectra (Figure 1, Table 1). The λ_{max} for the MLCT transition occurs at 371 nm ($\varepsilon = 6450\,\text{M}^{-1}\,\text{cm}^{-1}$) and 385 nm ($\varepsilon = 4430\,\text{M}^{-1}\,\text{cm}^{-1}$) for *N-trans*-[**1**-H]$^+$ and *C-trans*-[**1**-H]$^+$, respectively. Consistent with the large spin-orbit coupling constant of Ir, absorption bands or shoulders also appear at lower energy than the main peak from 450 to 550 nm for both hydrides owing to mixing of excited-state singlet and triplet charge-transfer states.[9] The calculated UV/Vis spectra for *N-trans*-[**1**-H]$^+$ and *C-trans*-[**1**-H]$^+$ using TDDFT display λ_{max} for the MLCT transition at 366 and 395 nm, respectively, consistent with the experimental spectra (Supporting Information, Figure S6). Also, calculations show that the lower absorption bands originate from excitations from Ir-ppy(d-π)-based orbitals to tpy. There is strong ppy-like character in the orbital from which excitation occurs.

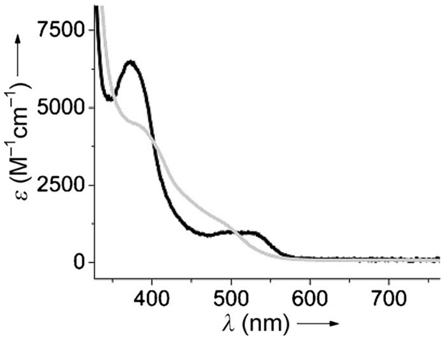

Figure 1. UV-vis spectra of *N-trans*-[**1**-H]$^+$ (black) and *C-trans*-[**1**-H]$^+$ (gray) in CH$_3$CN.

Table 1: Properties of geometric isomers of [**Ir**-H]$^+$.

	N-trans-[**1**-H]$^+$	*C-trans*-[**1**-H]$^+$
^{1}H NMR chemical shift of Ir-H (ppm)	−19.3	−7.46
UV-vis abs.: obsd (nm, M^{-1}cm^{-1})	371 (6450), 550 sh, 530	385 sh (4400), 500 sh
Calcd MLCT abs. (nm)	366	395
Measured $\Delta G°_{H^-}$ (kcal mol^{-1})	57	–
Calcd $\Delta G°_{H^-}$ (kcal mol^{-1})	53.7	43.2
Calcd Ir-H distance (Å)	1.62	1.73
Potentials in CH$_3$CN vs SCE (V)	1.14, −1.30, −1.60	–
Ground-state reactivity toward CO$_2$	No	Formation of *C-trans*-[**1**-OCHO]$^+$
Excited-state lifetime (ns)	176	112
Emission max (nm)	605	–
k_q by TEA (M^{-1}s^{-1})	1×10^8	No quenching, Ir-H cleavage

We performed DFT calculations in an attempt to investigate the different reactivity of *N-trans*-[**1**-X]$^{n+}$ and *C-trans*-[**1**-X]$^{n+}$ ($n = 1$ with X = H$^-$, Cl$^-$; $n = 2$ with X = CH$_3$CN) in the ground state. In the case of Cl$^-$ or CH$_3$CN bound to the Ir center, the *C-trans* isomers are more stable by 8.1 and 6.1 kcal mol^{-1}, respectively. Interestingly, *N-trans*-[**1**-H]$^+$ is favored by 4.4 kcal mol^{-1} compared to *C-trans*-[**1**-H]$^+$. As a result, the formation of *N-trans*-[**1**-H]$^+$ from the CH$_3$CN adduct is favored by 10.4 kcal mol^{-1} compared to *C-trans*-[**1**-H]$^+$, indicating the higher stability of *N-trans*-[**1**-H]$^+$ (Supporting Information, Scheme S1).

The CO$_2$ insertion reaction into the Ir-hydride bond to generate a metal-formato complex was investigated for both *N-trans*-[**1**-H]$^+$ and *C-trans*-[**1**-H]$^+$ isomers. After bubbling CO$_2$ into the CD$_3$CN solution of *N-trans*-[**1**-H]$^+$, no changes in the ^{1}H NMR spectrum were observed at RT or 70 °C (Supporting Information, Figure S7). However, immediate loss of the Ir-H proton peak at −7.46 ppm was observed with *C-trans*-[**1**-H]$^+$ while new peaks in the aromatic region appeared at room temperature (Supporting Information, Figure S8). The reactivity of *C-trans*-[**1**-H]$^+$ was further confirmed with ^{13}CO$_2$ (a new intense signal at 169.1 ppm with J(C,H) = 206 Hz; Supporting Information, Figure S9) and ESI-MS (Supporting Information, Figure S11), suggesting the generation of a formato species. The drastic difference in the CO$_2$ reactivity towards ground-state *N-trans*-[**1**-H]$^+$ and *C-trans*-[**1**-H]$^+$ is possibly due to the difference in their Ir−H bond strength and hydride donor ability, or hydricity (see below).

Next, we examined computationally the reactivity of *N-trans*-[**1**-H]$^+$ and *C-trans*-[**1**-H]$^+$ towards CO$_2$ and found that the formation of the formato complexes, *N-trans*-[**1**-OCHO]$^+$ and *C-trans*-[**1**-OCHO]$^+$, by CO$_2$ insertion into the Ir−H bond is endoergic by 14.6 and 2.0 kcal mol^{-1}, respectively. Such a difference in free-energy changes (ΔG_s) for a hydride transfer reaction to CO$_2$ stems from the greater stabilization of the hydride in *N-trans*-[**1**-H]$^+$ compared to other ligands (such as CH$_3$CN) and *C-trans*-[**1**-H]$^+$. We also located the transition state (TS) structure for the reaction with *C-trans*-[**1**-H]$^+$ (Supporting Information, Figure S12), which proceeds with an activation free energy ($\Delta G^{\neq}$) of 14.1 kcal mol^{-1}, consistent with the experimental observation of that reaction occurring even at room temperature. Despite all our efforts, we could not locate a similar TS for *N-trans*-[**1**-H]$^+$ as all structures investigated converged to the initial hydride complex, indicating that CO_2 insertion into *N-trans*-[**1**-H]$^+$ is not favorable in accord with the endoergic nature of the reaction.

Cyclic voltammograms of *N-trans*-[**1**-H]$^+$ in CH_3CN under Ar or CO_2 are shown in the Supporting Information (Figure S13). Under Ar, the *N-trans*-[**1**-H]$^+$ complex exhibits one reversible reduction of tpy at −1.30 V vs SCE (or −1.70 V vs $Fc^{+/0}$) followed by a small shoulder at −1.60 V. The oxidation of the iridium metal was observed at potential $E_p = 1.14$ V. Under a CO_2 atmosphere, a catalytic current peak was observed at the first reduction wave (ca. −1.30 V) with slightly increased current compared to that under Ar. A large catalytic current was observed before reaching −1.60 V. This result indicates that *N-trans*-[**1**-H]$^+$ also has electrocatalytic ability towards CO_2 reduction, which is similar to what was observed for [Ir(tpy)(ppy)Cl]$^+$ by Sato et al.[3] Experiments were also performed on *C-trans*-[**1**-H]$^+$ in acetonitrile, however, we could not obtain reliable data owing to its instability and the labile nature of its Ir−H bond.

The hydricities of transition-metal hydrides and their relation to CO_2 reduction activity have been well studied.[5,6] It is of interest to measure the thermodynamic hydricities of *N-trans*-[**1**-H]$^+$ and *C-trans*-[**1**-H]$^+$ in order to fully understand the CO_2 reduction mechanism. To determine the hydride donor ability of *N-trans*-[**1**-H]$^+$ and *C-trans*-[**1**-H]$^+$, we performed hydride-transfer reactions with an appropriate hydride acceptor of known hydride affinity. The reaction of *N-trans*-[**1**-H]$^+$ to hydride acceptors such as the BF_4 salts of tris(*p*-methoxyphenyl)trityl and 4-(acetylamino)-2,2,6,6-tetramethyl-1-oxo-piperidinium ($TEMPO^+$) through thermodynamic cycles provides the ground-state hydricity of $\Delta G°_{H^-} = 57 \pm 4$ kcal mol^{-1} in CH_3CN (see the Supporting Information). While there exists some ambiguity in the geometric change (*N-trans*-[**1**-H]$^+$ to *C-trans*-[**1**-$NCCH_3$]$^{2+}$), the observed hydricity of *N-trans*-[**1**-H]$^+$ is very similar to that of [CpRe^I-(NO)(CO)(CHO)] ($\Delta G°_{H^-} = 55$ kcal mol^{-1}).[6b] The relatively weak ground-state hydricity of *N-trans*-[**1**-H]$^+$ explains its stability and lack of reactivity towards CO_2 in the ground state. Efforts were also made to determine the ground-state hydricity of *C-trans*-[**1**-H]$^+$. We encountered difficulty in measuring the heat of reaction of *C-trans*-[**1**-H]$^+$ with tris(*p*-methoxyphenyl)trityl or $TEMPO^+$ owing to the instability of the hydride.

We also performed DFT calculations to predict the hydricity of *N-trans*-[**1**-H]$^+$ and *C-trans*-[**1**-H]$^+$, and to do so we calculated hydricities relative to the [Ru^{II}(tpy)-(bpy)H]$^+$/[Ru^{II}(tpy)(bpy)(CH_3CN)]$^{2+}$ couple for which the experimental hydricity is known ($\Delta G°_{H^-} = 39$ kcal mol^{-1}).[5b,6a] We calculated $\Delta G°_{H^-} = 53.7$ kcal mol^{-1} for *N-trans*-[**1**-H]$^+$, which is in good agreement with the experimentally determined value of $\Delta G°_{H^-} = 57$ kcal mol^{-1}. Using the same approach, we calculated $\Delta G°_{H^-} = 43.2$ kcal mol^{-1} for *C-trans*-[**1**-H]$^+$, displaying a similar hydricity to $HCOO^-$ (43 kcal mol^{-1}) and consistent with the experimental result of CO_2 insertion into its Ir−H bond.

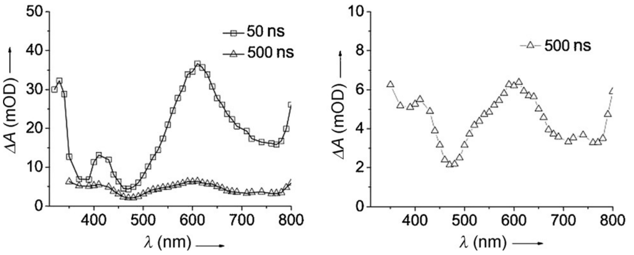

Figure 2. Left: Transient absorption spectra of *N-trans*-[**1**-H]$^+$ in the presence of 50 mM TEA at 50 ns (□) and 500 ns (△) in CH_3CN. Right: Expanded transient absorption spectrum of the product.

Excitation of *N-trans*-[**1**-H]$^+$ with λ_{exc} of 420 nm produces the ^{3}MLCT excited state and the transient absorption spectrum at 50 ns (Figure 2, left panel, black trace (□)), when the hydride is still in contact with the iridium metal atom, which features an absorption at 340 nm ascribed to a $\pi \rightarrow \pi^*$ transition. The excited state spectrum also reveals new transient absorption bands at 410 and 600 nm. The excited state lifetime of 176 ns (Supporting Information, Figure S16) is much shorter than those of *C-trans*-[**1**-Cl]$^+$ and *C-trans*-[**1**-$NCCH_3$]$^{2+}$ (2.2 and 2.6 μs, respectively; Supporting Information, Figure S17). The ^{3}MLCT excited state was quenched in the presence of a sacrificial electron donor such as triethylamine (TEA), yielding the one-electron-reduced species of *N-trans*-[**1**-H]$^+$ in CH_3CN where the added electron primarily resides in the tpy-π^*-orbitals. The quenching rate constant (k_q) of 1×10^8 M^{-1}s^{-1} (Supporting Information, Figure S18) is slower than that of *C-trans*-[**1**-Cl]$^+$ (3×10^9 M^{-1}s^{-1}; Supporting Information, Figure S19). To identify the product, we carried out Na-Hg reduction of *N-trans*-[**1**-H]$^+$ and *C-trans*-[**1**-$NCCH_3$]$^{2+}$ in CH_3CN (Supporting Information, Figures S20, S21). The spectra of the mono-reduced *N-trans*-[**1**-H]$^+$ and the doubly-reduced *C-trans*-[**1**-$NCCH_3$]$^{2+}$ species are identical indicating the formation of penta-coordinate [**1**]^0 on the time scale of Na-Hg reduction (10–20 min), presumably by forming 1/2 equiv of H_2. However, the transient spectrum at 500 ns (Figure 2, right panel) is slightly different from the difference spectrum of *N-trans*-[**1**-H]$^+$ and the OER species obtained by Na-Hg reduction (Supporting Information, Figure S21), indicating that the Ir−H bond may be intact on this time scale. In fact, the decay kinetics of this reduced species of *N-trans*-[**1**-H]$^+$ was not influenced by the presence of CO_2 up to 50 ms (Supporting Information, Figure S23). However, as mentioned earlier, the CV under CO_2 exhibits a catalytic current after passing the first reduction potential, indicating that [**1**]^0 formed by the Ir−H bond cleavage is reactive toward CO_2.

The decay of the excited-state of *C-trans*-[**1**-H]$^+$ obeys pseudo-first-order kinetics with a lifetime of about 112 ns (Supporting Information, Figure S24). The initial excited-state spectrum of *C-trans*-[**1**-H]$^+$ at 50 ns is shown in Supporting Figure S25 (black trace). No peak at 410 nm was observed for *C-trans*-[**1**-H]$^+$. The ^{3}MLCT excited-state could not be quenched with TEA. Furthermore, the bulk photolysis of *C-trans*-[**1**-H]$^+$ in CD_3CN monitored by ^{1}H NMR exhibits the immediate loss of the hydride proton to form the penta-coordinate [**1**]^0 species (Supporting Information, Figure S27).

The ^{3}MLCT excitation reduces the electron donor ability of the iridium metal center and enhances the release of the proton as a photoacid. This type of photoinduced excited-state deprotonation has also been observed in other iridium hydride complexes.[10] It should be noted that *N-trans*-[**1**-H]$^+$ was produced with approximately 40 % yield after a prolonged 10 min bulk photolysis, indicating that the protonation of [**1**]^0 occurs to generate the stable isomer (Supporting Information, Figure S27).

We explored photocatalytic CO_2 reduction using both hydride isomers under visible light irradiation (> 410 nm) in the presence of the sacrificial electron donor TEOA (Figure 3). Both hydrides show similar TONs of about 45 for CO production. Small amounts of H_2 and HCOOH were also produced during photocatalytic CO_2 reduction by the hydrides. The similar efficiency and TON of photochemical CO formation by both hydrides and [**1**-Cl]$^+$ indicate that the actual photocatalytic reaction occurs through a common penta-coordinate [**1**]^0 intermediate. We investigated computationally the generation of [**1**]^0 from both hydride isomers and the mechanism of CO_2 reduction with [**1**]^0 as the key intermediate. The proposed pathways for CO generation are summarized in Scheme 2. An interesting feature of the proposed mechanism is that only the *C-trans*-[**1**]^0 isomer exists in the ground state and is the key reactive species. Detailed theoretical results are described in the Supporting Information.

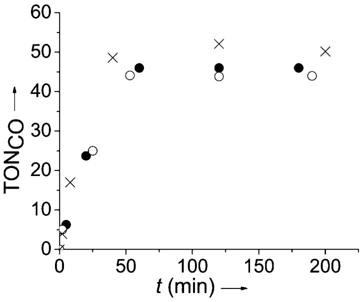

Figure 3. Photocatalytic CO formation with 0.5 mM *N-trans*-[**1**-H]$^+$ (●), *C-trans*-[**1**-H]$^+$ (○), and *C-trans*-[**1**-Cl]$^+$ (×) in CH_3CN/TEOA (5:1) under CO_2 atmosphere.

In conclusion, we have investigated using experimental and computational methods the interaction of CO_2 with [**1**-H]$^+$, which was previously proposed as the key intermediate during the reduction of CO_2. We find that only one isomer, *C-trans*-[**1**-H]$^+$, reacts with CO_2 to generate the formato complex at room temperature. Under irradiation, this hydride acts as a photoacid to produce penta-coordinate *C-trans*-[**1**]^0, which is involved in the photocatalytic reduction of CO_2 to CO. The other hydride isomer, *N-trans*-[**1**-H]$^+$, does not react with CO_2 at room temperature, or even at higher temperatures, to generate the formato complex whereas during the photocatalytic CO_2 reduction cycle with an electron donor, penta-coordinate C-*trans*-[**1**]^0 (to the vacant site) is formed to generate CO from CO_2. The proposed mechanism for photochemical CO_2 reduction (Scheme 2) (see the Supporting Information for a detailed description of the proposed mechanism) features a common reactive *C-trans*-[**1**]^0 species irrespective of the starting isomer or ligand (for example, hydride or CH_3CN). The presence of only one isomer, namely *C-trans*-[**1**]^0, as a penta-coordinate complex at the formal Ir^I oxidation state is a quite interesting observation and will have profound implications in future ligand design for CO_2 reduction catalysts. We have also compared the ground-state hydricities of these two isomers. Our evaluation of the hydricities and understanding of mechanism of CO_2 photoreduction should help in further developments in this area. We are currently investigating more details of the CO_2 reaction with [**1**]^0 and the subsequent reactions.

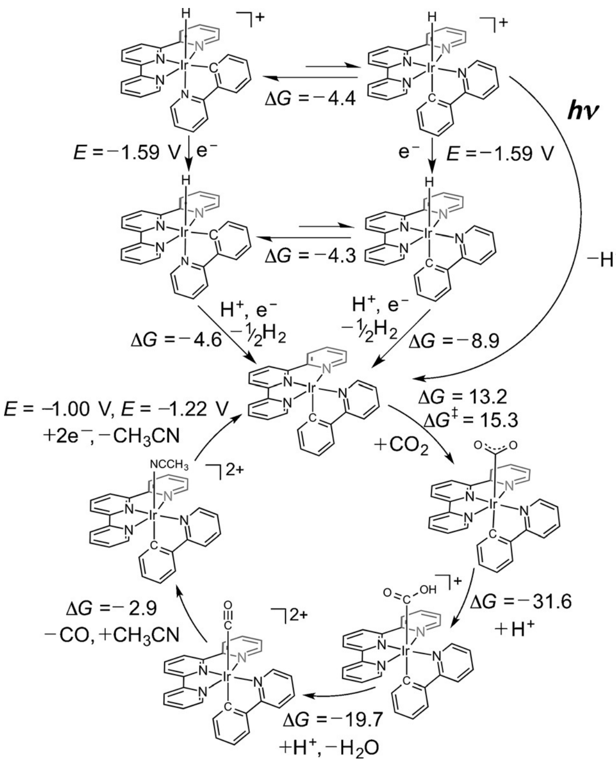

Scheme 2. Possible mechanism for photocatalytic CO_2 reduction with [**1**-H]$^+$. Unit of ΔG: kcal mol^{-1}.

Experimental Section

The starting complexes [Ir(tpy)Cl_3] and [**1**-Cl]$^+$ were prepared according to the previously reported literature procedures.[3,11] The complexes [**1**-OH_2]$^{2+}$ and [**1**-$NCCH_3$]$^{2+}$ were prepared by the Cl$^-$ ligand replacement from [**1**-Cl]$^+$ by using water or acetonitrile as the solvent. [**1**-Cl]$^+$, [**1**-OH_2]$^{2+}$, and [**1**-$NCCH_3$]$^{2+}$ were found to have the monodentate ligand *trans* to C of ppy, therefore, we do not specify the geometries thereafter. The synthesis procedure, NMR, ESI-MS, UV/Vis, and elemental analysis of *N-trans*-[**1**-H](PF_6) and *C-trans*-[**1**-H](PF_6) are summarized in the Supporting Information. The detailed procedures and the results of the following experiments are presented in the supporting information: ground- and excited-state chemistry; electrochemistry; reactions with CO_2; X-ray structure of *N-trans*-[**1**-H]$^+$; theoretical and experimental determination of the hydricities; and DFT calculations of various Ir species to determine the possible CO_2 reduction mechanism.

CCDC 1415385 contains the supplementary crystallographic data for this paper. These data can be obtained free of charge from The Cambridge Crystallographic Data Centre.

Acknowledgements

We thank Drs. Dmitry Polyansky and Gerald Manbeck for valuable discussions. The work carried out at Brookhaven National Laboratory was supported by the U.S. Department of Energy, Office of Science, Division of Chemical Sciences, Geosciences, & Biosciences, Office of Basic Energy Sciences under contract DE-SC00112704. Y.M. and S.S. thank the Japan Science and Technology Agency (JST) for a part of the financial support.

Keywords: CO_2 reduction · homogeneous catalysis · hydricity · iridium hydrides · photochemistry

How to cite: *Angew. Chem. Int. Ed.* **2015**, *54*, 14128–14132
Angew. Chem. **2015**, *127*, 14334–14338

[1] a) S. Berardi, S. Drouet, L. Francas, C. Gimbert-Surinach, M. Guttentag, C. Richmond, T. Stoll, A. Llobet, *Chem. Soc. Rev.* **2014**, *43*, 7501; b) Y. Izumi, *Coord. Chem. Rev.* **2013**, *257*, 171; c) L. Hammarström, S. Hammes-Schiffer, *Acc. Chem. Res.* **2009**, *42*, 1859; d) Y. Oh, X. Hu, *Chem. Soc. Rev.* **2013**, *42*, 2253.

[2] a) J. Hawecker, J.-M. Lehn, R. Ziessel, *J. Chem. Soc. Chem. Commun.* **1983**, 536; b) E. Fujita, *Coord. Chem. Rev.* **1999**, *185–186*, 373; c) A. J. Morris, G. J. Meyer, E. Fujita, *Acc. Chem. Res.* **2009**, *42*, 1983; d) H. Takeda, O. Ishitani, *Coord. Chem. Rev.* **2010**, *254*, 346; e) H. Takeda, K. Koike, T. Morimoto, H. Inumaru, O. Ishitani, *Adv. Inorg. Chem.* **2011**, *63*, 137.

[3] S. Sato, T. Morikawa, T. Kajino, O. Ishitani, *Angew. Chem. Int. Ed.* **2013**, *52*, 988; *Angew. Chem.* **2013**, *125*, 1022.

[4] R. O. Reithmeier, S. Meister, B. Rieger, A. Siebel, M. Tschurl, U. Heiz, E. Herdtweck, *Dalton Trans.* **2014**, *43*, 13259.

[5] a) M. Rakowski DuBois, D. L. DuBois, *Acc. Chem. Res.* **2009**, *42*, 1974; b) Y. Matsubara, E. Fujita, M. D. Doherty, J. T. Muckerman, C. Creutz, *J. Am. Chem. Soc.* **2012**, *134*, 15743; c) C. Creutz, M. Chou, *J. Am. Chem. Soc.* **2007**, *129*, 10108; d) S. M. Barrett, C. L. Pitman, A. G. Walden, A. J. M. Miller, *J. Am. Chem. Soc.* **2014**, *136*, 14718.

[6] a) J. T. Muckerman, P. Achord, C. Creutz, D. E. Polyansky, E. Fujita, *Proc. Natl. Acad. Sci. USA* **2012**, *109*, 15657; b) W. W. Ellis, A. Miedaner, C. J. Curtis, D. H. Gibson, D. L. DuBois, *J. Am. Chem. Soc.* **2002**, *124*, 192.

[7] H. Konno, A. Kobayashi, K. Sakamoto, F. Fagalde, N. E. Katz, H. Saitoh, O. Ishitani, *Inorg. Chim. Acta* **2000**, *299*, 155.

[8] Y. Zhao, D. G. Truhlar, *Theo. Chem. Acc.* **2008**, *120*, 215.

[9] M. G. Colombo, A. Hauser, H. U. Guedel, *Inorg. Chem.* **1993**, *32*, 3088.

[10] T. Suenobu, D. M. Guldi, S. Ogo, S. Fukuzumi, *Angew. Chem. Int. Ed.* **2003**, *42*, 5492; *Angew. Chem.* **2003**, *115*, 5650.

[11] T. Yutaka, S. Obara, S. Ogawa, K. Nozaki, N. Ikeda, T. Ohno, Y. Ishii, K. Sakai, M. Haga, *Inorg. Chem.* **2005**, *44*, 4737.

Received: July 27, 2015